

Upper ocean response to Typhoon Choi-Wan as measured by the Kuroshio Extension Observatory mooring

Nicholas A. Bond,¹ Meghan F. Cronin,² Christopher Sabine,² Yoshimi Kawai,³ Hiroshi Ichikawa,³ Paul Freitag,² and Keith Ronnholm¹

Received 2 August 2010; revised 4 November 2010; accepted 20 December 2010; published 22 February 2011.

[1] The Kuroshio Extension Observatory (KEO) is a highly instrumented moored reference station located at 32.3°N, 144.5°E in the recirculation gyre south of the Kuroshio Extension. On 19 September 2009, the eye of Typhoon Choi-Wan (International designation: 0914) passed ~40 km to the southeast of the KEO surface mooring. Hourly meteorological and physical oceanographic measurements together with 3 hourly air-sea carbon dioxide observations telemetered from KEO in near real time show the evolution of the upper ocean and its associated air-sea fluxes during the passage of this storm and its aftermath. During the approach of the storm, the mixed layer freshened because of intense rainfall. This was followed by a large outgassing of CO₂, rapid cooling, and an increase in salinity. Although these changes in mixed layer properties imply substantial entrainment, they were accompanied by upwelling and ultimately a temporary ~20 m shoaling of the mixed layer. This upwelling, which was observed at all depths, including the deepest sensor near 500 m, was coincident with the onset of near-inertial oscillations in the mixed layer currents. After the typhoon passed, inertial pumping caused ~15–20 m amplitude vertical displacements throughout the top 500 m that continued for at least 6 days. A large oceanic response was observed in this case even though the eye of Choi-Wan passed to the right of KEO, resulting in winds rotating cyclonically with time, in opposition to the anticyclonic-rotating near-inertial currents.

Citation: Bond, N. A., M. F. Cronin, C. Sabine, Y. Kawai, H. Ichikawa, P. Freitag, and K. Ronnholm (2011), Upper ocean response to Typhoon Choi-Wan as measured by the Kuroshio Extension Observatory mooring, *J. Geophys. Res.*, 116, C02031, doi:10.1029/2010JC006548.

1. Introduction

[2] It is widely appreciated that tropical cyclones represent strong forcing events for the upper ocean, as evidenced by satellite observations of substantial decreases in sea surface temperature (SST) in the cyclones' wakes. These wakes are not restricted to a narrow path along the storm center's path but rather can occur in a swath hundreds of kilometers wide, as illustrated in Figure 1 for the present case, Typhoon Choi-Wan in September 2009 (International designation: 0914). The cooling of the upper ocean has a variety of implications. First, this cooling serves to reduce the air-sea temperature and hence the fluxes of enthalpy, thereby influencing the evolution of the storm itself, and the formation and evolution of subsequent storms (see the work of *Bender et al.* [1993], among many others). The other implications may be less obvious. As discussed by *Emanuel*

[2001] and *Sriver and Huber* [2010], the upper ocean mixing with these storms impacts the vertical distribution of heat, and ultimately meridional heat transports. In this way, tropical cyclones help drive the poleward flux of heat and thereby the thermohaline circulation and global climate. Moreover, these storms may represent an important contribution to the net air-sea flux of CO₂ of the subtropical oceans [*Bates et al.*, 1998a]. Therefore, from both weather forecasting and climate perspectives, it is important to better document how the upper ocean responds to these intense events.

[3] Subsurface measurements of the oceanic response to tropical cyclones are sparse, however, since these events are highly episodic and rare for any specific location. In particular, while there have been a number of investigations of the before and after oceanic conditions associated with Atlantic hurricanes based on expendable profilers [e.g., *Sanford et al.*, 1987], these have been limited to snapshots. A well-instrumented buoy with a high data collection rate is the most effective way to fully document the temporal evolution of the ocean to the approach, passage and departure of a storm. Previous case studies from the Atlantic Ocean [*Dickey et al.*, 1998], the East China Sea [*Nemoto et al.*, 2009], and the Indian Ocean [*McPhaden et al.*, 2009], include observations of a variety of ocean responses

¹Joint Institute for the Study of the Atmosphere and Ocean, University of Washington, Seattle, Washington, USA.

²Pacific Marine Environmental Laboratory, NOAA, Seattle, Washington, USA.

³Japan Agency for Marine-Earth Science and Technology, Yokosuka, Japan.

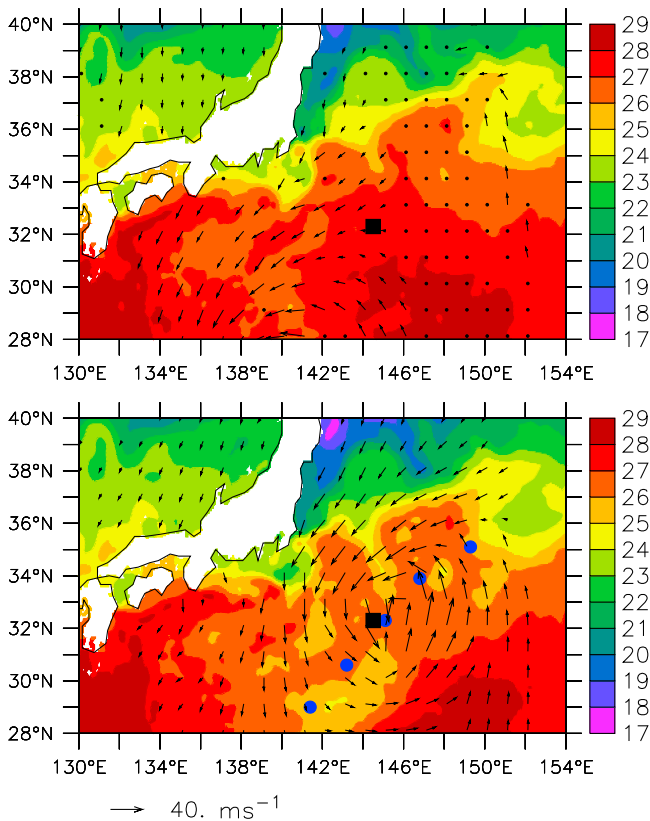


Figure 1. Surface winds (vectors) from Jet Propulsion Laboratory's SeaWinds QuikSCAT Level 3 swath data set, and daily averaged sea surface temperature (color fill) from the Global Ocean Data Assimilation Experiment (GODAE) high-resolution sea surface temperature (SST) data set for approximately 0000 UTC on (top) 19 September and on (bottom) 20 September. The black square indicates the location of the Kuroshio Extension Observatory (KEO) mooring. The blue dots represent approximate positions of the surface low center at 6 h intervals between 0600 UTC 19 September and 0600 UTC 20 September.

to the passage of tropical cyclones but none of these studies had the number and variety of sensors available on the Kuroshio Extension Observatory (KEO) mooring.

[4] The KEO surface mooring is a reference station mooring deployed at 32.3°N, 144.5°E in the recirculation gyre south of the Kuroshio Extension [Cronin *et al.*, 2008]. KEO is instrumented to monitor air-sea fluxes of heat, moisture, momentum, and carbon dioxide; temperature and salinity down to 525 m; and near-surface currents (see Appendix A). The oceanography of the region includes considerable mesoscale energy and occasionally strong mean currents in association with southward displacements of the Kuroshio Extension. A well-defined seasonal thermocline exists between typically 50 and 100 m in the late summer and fall. Below this layer is North Pacific subtropical mode water (STMW) [Hanawa and Suga, 1995] of high salinity, low-density stratification, and high dissolved inorganic carbon (DIC) and CO₂ partial pressure (*p*CO₂). Although KEO is located at a latitude where tropical cyclones typically begin to make their extratropical transition

[e.g., Bond *et al.*, 2010], these storms can still be intense. In particular, the eye of Typhoon Choi-Wan was well defined as it passed 40 km to the southeast (i.e., to the right) of KEO on 19 September 2009 (Figures 1–2). This case study thus provides a useful contrast to the study of Dickey *et al.* [1998] of the response to Hurricane Felix, which passed to the left of the Bermuda Testbed Mooring (BTM). For cyclones in the Northern Hemisphere, winds in these locations rotate anticyclonically with time and thus can resonate with the currents with near-inertial oscillations, while on the other side of the track of a storm's low center (e.g., at KEO during Choi-Wan), the winds rotate cyclonically, and thus counter to these currents. As discussed by Price *et al.* [1994] among others, near-inertial internal waves represent a primary mechanism through which storm-forced currents in the mixed layer impact the thermocline and deeper waters and their resonant forcing causes the oceanic response in the wake of the typhoon to be strongest to the right of the eye's path. Thus one might expect that the response described by Dickey *et al.* [1998] would be more dramatic than found at KEO, all else being similar. We will show, however, that while the response was slightly less than seen at BTM, the inertial oscillations were relatively strong, due in part to the asymmetry of the storm as it passed the mooring. The present case will also be compared to the study of Nemoto *et al.* [2009], which considered atmospheric and oceanic CO₂ observations from a mooring during the passage of three typhoons (one that passed essentially overhead, one that passed 300 km to the left, and one that passed 300 km to the right). Scale parameters are provided here for purposes

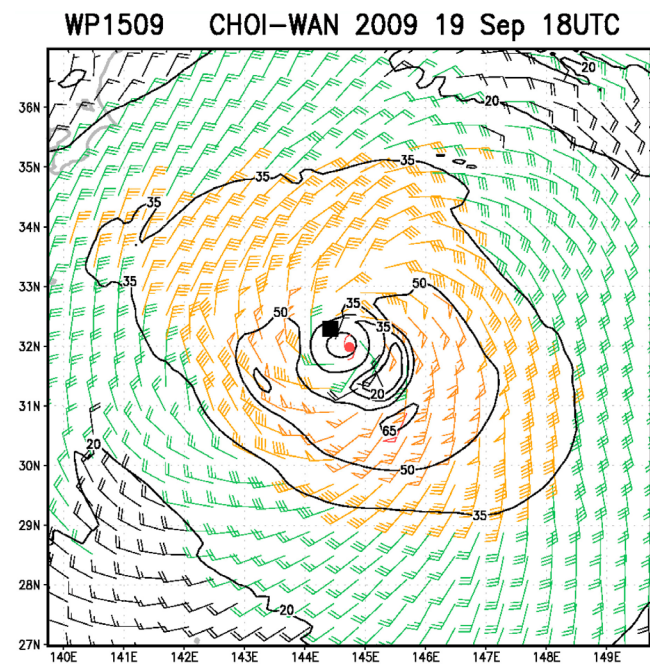


Figure 2. Estimated surface winds (knots) at 1800 UTC 19 September from the multiplatform tropical cyclone surface wind analysis from the Regional and Mesoscale Meteorology Branch of NOAA/NESDIS Center for Satellite Applications and Research. The black square indicates the approximate location for the KEO mooring.

of comparison with other studies of the ocean's response to tropical cyclones.

2. Review of Weather and Measurement Systems

[5] The disturbance that became Typhoon Choi-Wan was identified as a tropical depression on 12 September 2009 by the Joint Tropical Warning Center (JTWC). The storm intensified rapidly and became a category 5 super typhoon by 16 September with an estimated central sea level pressure (SLP) of 917 hPa and peak sustained winds of 71 m s^{-1} . It reached its westernmost point early on 18 September and then began propagating to the northeast. It had a forward speed of $U_H \sim 11 \text{ m s}^{-1}$ (based on the track from JTWC) as it passed $\sim 40 \text{ km}$ to the southeast of KEO at approximately 1800 UTC 19 September as a category 1 typhoon. A regional perspective of the SST and winds as Choi-Wan approached KEO, and a short time after its passage, is shown in Figure 1. There was a relatively homogeneous distribution of SST south of 34°N prior to the storm. As indicated by the change in SST illustrated in Figure 1, Choi-Wan caused surface cooling that was enhanced along a pair of swaths, with one displaced to the northwest of the track of the low center and the other to the southeast of the track.

[6] A higher-resolution analysis of the winds at 1800 UTC 19 September near the time of the closest approach of the storm to KEO is shown in Figure 2. Choi-Wan was then in the early stages of its transition to an extratropical cyclone, and had already become asymmetric. The distribution of the wind at this time included a local minimum in speed just to the southeast of the storm center, and in general, lower speeds to the north than to the other sides of the storm center. KEO experienced the strong tangential winds associated with the vestiges of the cyclone's eyewall; the combination of cyclonic curvature and horizontal shear implies intense positive wind stress curl. The corresponding Ekman pumping caused upwelling within at least the upper 500 m, as will be shown below. The passage of the storm center to the right of KEO caused the winds to blow first from the northeast and then from the northwest. This counterclockwise (cyclonic) shift in the wind direction with time is opposite to the sense of turning of inertial currents, as mentioned earlier. Nevertheless, as will be shown below, Choi-Wan's strong winds did result in substantial impacts on the upper ocean including near-inertial internal waves and inertial pumping.

[7] For this analysis, we use data from the KEO mooring, including hourly meteorological data for computing the bulk air-sea heat, moisture, and momentum fluxes [Fairall *et al.*, 2003; Kubota *et al.*, 2008], 3 hourly sea-air $p\text{CO}_2$ from a PMEL MAPCO₂ surface ocean and atmospheric CO₂ measurement package similar to the one described by Shellito *et al.* [2008], hourly temperature from 20 sensors in the upper 525 m, hourly salinity from 11 sensors in the upper 525 m, and hourly near-surface (15 m) currents. Because of the strong currents in this region, the KEO mooring is of slackline design with a scope of 1.4. Thus the temperature and salinity data from all subsurface sensors were remapped onto constant depth surfaces using the pressure data from the sensors. Details of the KEO mooring system used in 2004–2006 are given by Cronin *et al.* [2008]. The mooring was updated in 2007 to make it more robust to

the harsh conditions found in the Kuroshio Extension. These modifications are described in Appendix A.

[8] As shown in Figure 3, indications of the impending typhoon could be seen in the reduction of solar radiation because of clouds late on 18 September. Less than 24 h later, on 19 September at 1800 GMT, the SLP reached a minimum of 955 hPa, coinciding with a burst of rainfall and a shift from east-northeasterly winds of 20 m s^{-1} during the storm's approach, to northwesterly winds of $20\text{--}30 \text{ m s}^{-1}$ during its departure. The latter interval included the peak wind gust of 41 m s^{-1} . The time series of the winds at KEO, and the wind analysis shown in Figure 2, indicate that the positive wind stress curl and local Ekman upwelling at KEO was primarily over the period of 1500 to 2000 GMT on 19 September. This timing is relevant to interpretation of the oceanographic observations presented below.

[9] The wind shift was accompanied by a decrease in the precipitation as measured by the R. M. Young capacitance rain gauge from rates of $\sim 10 \text{ mm h}^{-1}$ to $< 1 \text{ mm h}^{-1}$ late on 19 September. There was a 3 h data gap earlier on 19 September; we expect there was considerable rain during that interval based on the salinity observations presented later. We are unaware of previous studies of tropical cyclones reporting direct observations of precipitation rates over the open ocean. The peak hourly rate of $\sim 15 \text{ mm h}^{-1}$ observed at KEO by the R.M. Young rain gauge compares quite well with the mean rain rate of $\sim 18 \text{ mm h}^{-1}$ in hurricane rainbands found by Marks *et al.* [1993] based on airborne radar measurements. It should be noted that this KEO rain gauge measurement includes the correction of Serra *et al.* [2001] for wind effects based on the work of Koschmieder [1934].

[10] The sum of the surface sensible and latent heat fluxes increased rapidly to over 800 W m^{-2} with the onset of the winds from the northwest. This increase is due to the relatively cool and dry air to the west of the storm center, and is a sign of the asymmetry, and the early stage of Choi-Wan's extratropical transition, mentioned earlier. By way of comparison, Jacob *et al.* [2000] reported peak combined heat fluxes of $\sim 1200 \text{ W m}^{-2}$ in association with Hurricane Gilbert. For the present case, the average rate of net heat loss at the surface was $\sim 390 \text{ W m}^{-2}$ for the 24 h period beginning 1900 UTC 19 September, corresponds to a cooling rate of less than 0.2°C per day distributed over the top 50 m, which is the approximate depth of the mixed layer prior to the event. The mixed layer experienced a drop in temperature of $\sim 0.7^\circ\text{C}$ during this period reflecting both the heat loss to the atmosphere and the introduction of cooler water from below.

[11] September is a transition period for the KEO region from summer time supersaturated carbon dioxide levels to the winter undersaturated values. As sea surface temperatures cool, the surface water $p\text{CO}_2$ decreases by 4.23% per degree Celsius decrease in temperature because of a redistribution of the dissolved carbon species [Takahashi *et al.*, 1993]. Prior to the storm, KEO surface waters were a small source of CO₂ to the atmosphere with the water minus air values ($\Delta p\text{CO}_2$) of about $10\text{--}20 \mu\text{atm}$ (Figure 2). As the storm passed the site, surface water $p\text{CO}_2$ increased dramatically giving a maximum $\Delta p\text{CO}_2$ of nearly $55 \mu\text{atm}$. There was a relaxation in this pressure difference to the prestorm conditions of $10\text{--}20 \mu\text{atm}$ in the 12 h following the storm, and then a slow decrease in the oceanic $p\text{CO}_2$ until

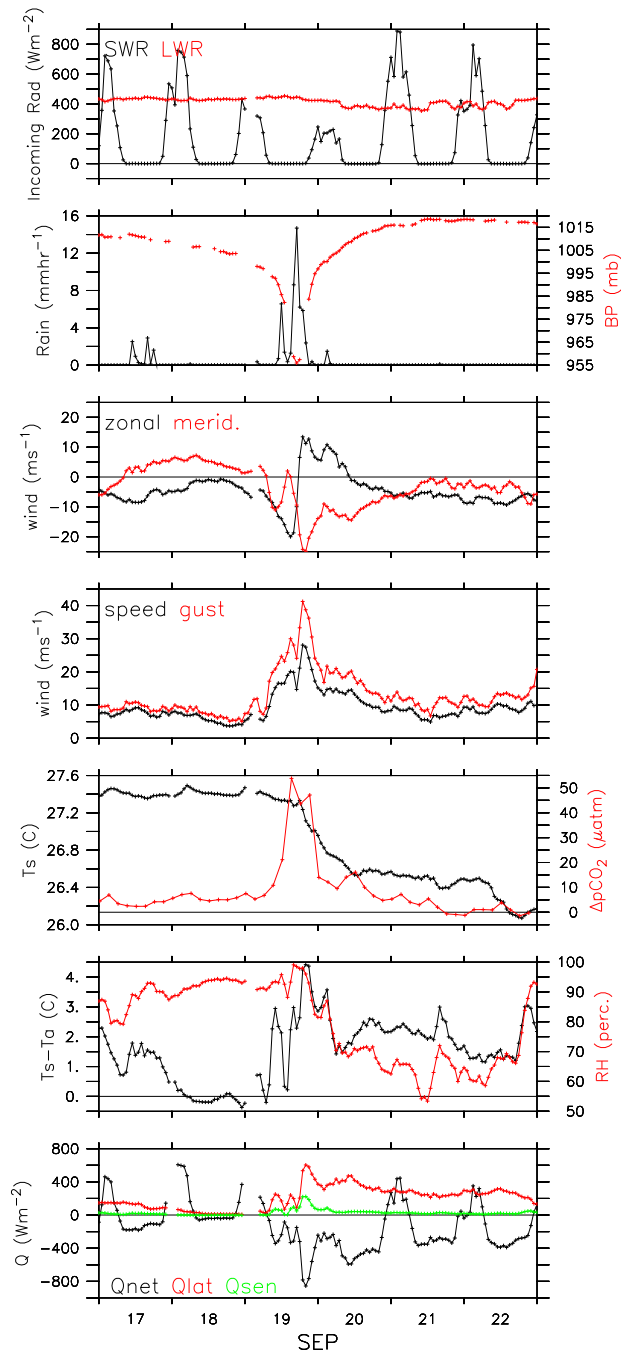


Figure 3. Hourly time series of air-sea interaction parameters observed at KEO for 17–22 September 2009, except for $\Delta p\text{CO}_2$, which is 3 hourly. From top to bottom, the sets of traces indicate the downward shortwave radiation (black) and longwave radiation fluxes (red); rain rate (black) and barometric pressure (red); zonal (black) and meridional (red) components of the wind; average wind speed (black) and peak gust (red); SST (black) and $\Delta p\text{CO}_2$ (red); sea-air temperature difference (black) and atmospheric relative humidity (red); net surface heat flux (black), surface latent heat flux (red), and surface sensible heat flux (green). The units are indicated with the scales on the sides of the panels. The winds are based on 6 bursts of data of 2 min duration each hour, and the gusts are peak values of 3 s averages of the speeds during each set of bursts.

the surface ocean was a small sink for CO_2 approximately 5 days after the storm.

3. Evolution of Upper Ocean Conditions

[12] The evolution of the upper portion of the water column during the passage of Choi-Wan, and its aftermath, was well-sampled by KEO. Here we first illustrate the oceanographic response during the storm itself through time depth sections of temperature and salinity for a 6 day period (17–22 September) encompassing the storm (Figure 4). The most rapid cooling of the upper portion of the water column began late on 19 September continuing into early the next day. This cooling coincided with marked shoaling of the base of the mixed layer and began during the northwesterly

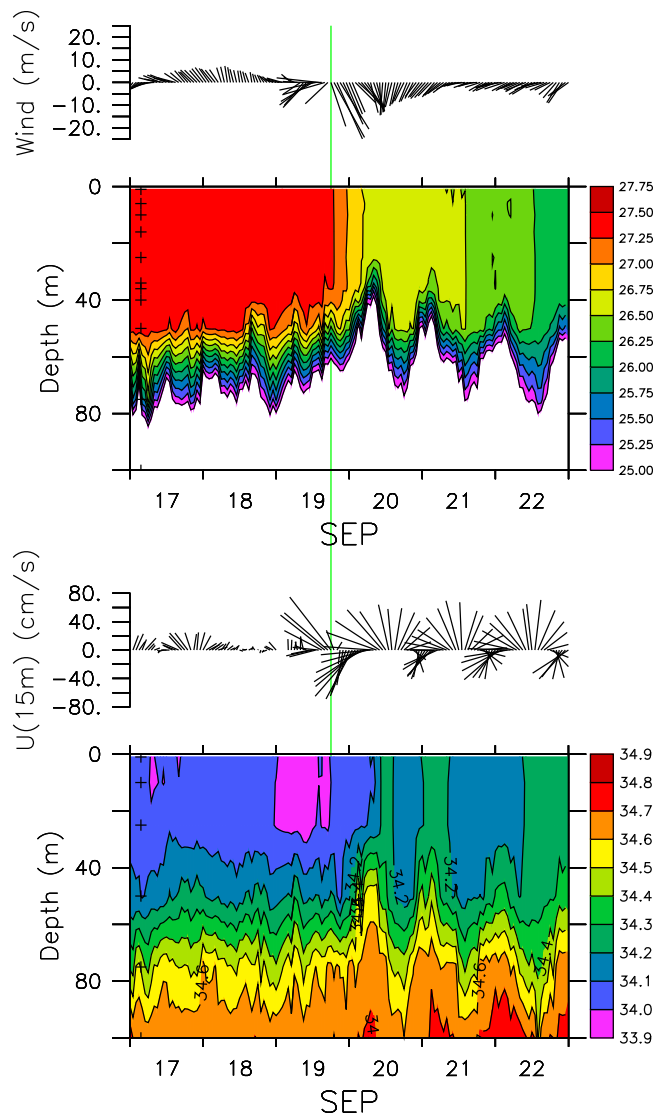


Figure 4. (top) Time depth sections of hourly temperature with surface winds and (bottom) salinity with 15 m currents from KEO for the period 17–22 September. The 15 m currents are plotted every 2 h. The nominal depths of the sensors are shown as plus marks near the start of the time series. The green vertical line marks the time of the primary wind shift at 1800 UTC 19 September.

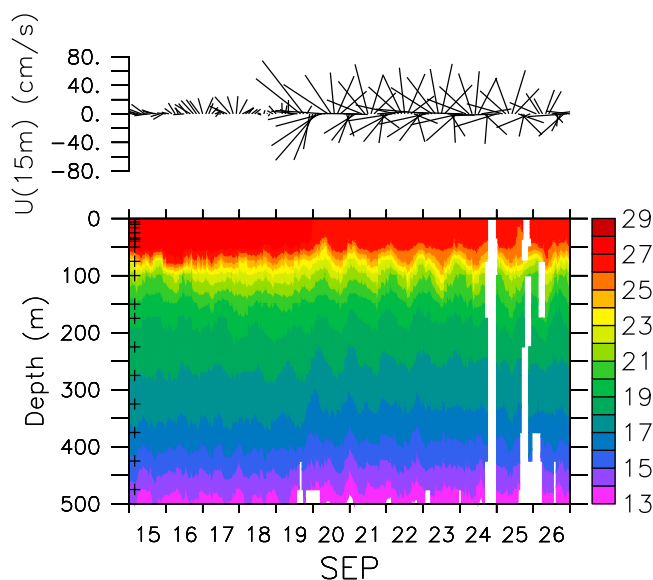


Figure 5. Time depth section of temperature (C) from KEO (color scale at right; contour interval 0.5 C). The nominal depths of the sensors are shown as plus marks near the start of the time series.

winds after the closest passage of the SLP low center. An important point here is that this upwelling, and thermal response, occurred after the main wind shift and implied wind stress curl, as indicated by the time series of the winds shown in Figure 4 (top). As a consequence, the mixed layer was thinnest at around 0600 UTC on 20 September. After this period of direct forcing by the typhoon, the mixed layer started to slowly thicken while also experiencing the pumping associated with internal near-inertial waves. The period from 20 to 22 September also included a slow cooling of the mixed layer, and a vertical spreading in the isotherms in the 25°–26°C range, i.e., a decrease in the thermal stratification in the upper portion of the thermocline. Similarly, *Maeda et al.* [1996] documented the onset of prominent near-inertial oscillations with a sudden decrease in the winds associated with a typhoon.

[13] The sudden rise in $\Delta p\text{CO}_2$ with the storm seen in Figure 3 is likewise consistent with the onset of vigorous entrainment into the mixed layer of water with high $p\text{CO}_2$. The subsequent drop in $p\text{CO}_2$ in the surface waters on 20 September implies a marked decrease in the rate of entrainment relative to the effects of cooling because of the loss of heat at the surface, and secondarily, the outgassing at the sea surface. We note that there appeared to be a continuance of the mixing within the thermocline during this interval, leading to reduced stratification in that layer as noted above. As the mixed layer continued to cool in the days following the storm the $p\text{CO}_2$ changed following the thermodynamic response.

[14] With regards to salinity, rainfall apparently occurred early on the 19th, as reflected by the temporary freshening of the upper 30 m (there was a short gap in the rainfall record). The salinity in this layer then increased by about 0.3 psu over approximately the next day because of the inferred entrainment driven by mixing. The inertial pumping that began on 20 September indicated in the temperature

time series is also evident in the salinity. On the basis of the vertical displacements of the 34.5 isohaline, the amplitude of these waves was 12–15 m. During 20 and 21 September, there was a lag of a few hours between the upward heaves in the isohalines below the mixed layer and temporary maxima in salinity in the upper 40 m. The freshening on 20 and 21 September does not appear to be due to rainfall, but instead to advection by the horizontal component of the near-inertial currents (shown on top of the lower panel in Figure 4), i.e., sloshing of water back and forth with different salinity. *D'Asaro et al.* [2007] discuss the effect of this mechanism on upper ocean heat content. The horizontal variations in salinity responsible for these fluctuations appear to be largely due to spatial differences in the rainfall associated with Choi-Wan. The background state of the upper ocean in the vicinity of KEO includes higher salinity to the south, but given the measured currents, the gradient in salinity (based on the Levitus climatology) is insufficient to produce the magnitude of the temporal changes observed at KEO. The amplitude of the inertial pumping declined only slowly with time, as shown in a time height section of temperature for the period from 15 through 26 September (Figure 5).

[15] The subtropical mode water (STMW) at KEO (the layer of reduced thermal stratification between about 150 to 350 m) also began experiencing more prominent vertical displacements on 19 September (Figure 5). To the extent that the isotherms represent material surfaces, the vertical amplitudes of the near-inertial waves in this layer were greater in the lower portion of this layer, as can be seen in the trace for the 18°C isotherm that ranges in depth between about 250 and 290 m. This may be attributed to the reduced static stability below the salinity maximum that lies at and above the STMW layer (not shown). The vertical oscillations featured more complex and higher-frequency structures with time after the storm, reflecting the growing presence of higher-order modes [*Gill*, 1984]. The time depth section of temperature also indicates a rather sudden increase in thermal stratification in the lower portion of the STMW late on 19 September shortly after the passage of the storm. This stratification appears to be caused by the overall cooling at depth apparently because of upwelling, while the temperature at the base of the seasonal thermocline remained relatively steady presumably because of compensation between the downward mixing of heat and upwelling of cool water (Figure 6). The STMW is usually effectively insulated from the atmospheric forcing at this time of year. By increasing the stratification of the STMW, extreme events such as Choi-Wan can impact the MLD that develops in the following winter [*Qiu and Chen*, 2006; *Kako and Kubota*, 2007].

[16] There are interesting differences in the timing of the primary changes in mixed layer temperature, salinity and $\Delta p\text{CO}_2$ during the passage of Choi-Wan. The sharp rise in $\Delta p\text{CO}_2$ preceded the main drop in temperature by about 6 h, which itself occurred about 9 h before the most rapid increase in salinity. This sequence could be explained if the Ekman pumping brought up water from near the base of the mixed layer that was relatively high in CO_2 but not much colder than the surface waters, followed by entrainment of colder water from well within the seasonal thermocline. This cooling was initially accompanied by only a modest increase

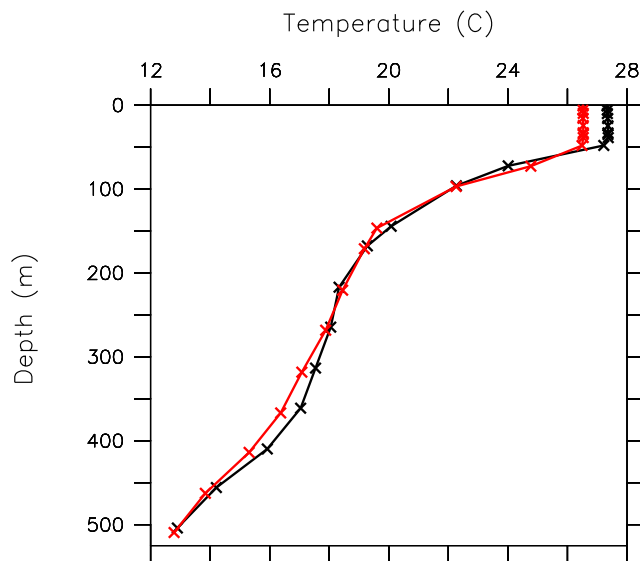


Figure 6. Temperature profiles at 1200 UTC 19 September (black line) and 1200 UTC 21 September (red line). The depths at which the temperature sensors were located at each time are indicated with x's.

in the salinity in the upper part of the water column because of rainfall. The later increase in salinity occurred during a period of northward near-inertial currents.

[17] The meteorological and upper ocean measurements collected at KEO have been used to carry out a scale analysis of the mixed layer momentum during the period of strongest wind forcing. The purpose here is to determine how well the forcing in this case, which was more impulsive than resonant with the rotation associated with near-inertial flows, corresponds with the observed mixed layer currents. The wind shifted at about 1800 UTC 19 September from out of the east-northeast to out of the northwest. The first two hours of the northwesterly winds coincided with a decline in the current speeds measured in the upper 15 m from about 0.6 m s^{-1} to 0.25 m s^{-1} . This deceleration can be attributed to the opposition of the winds to the currents generated prior to the primary wind shift, since the inertial rotation of these currents was counter to that in the winds. From 2000 to 2300 UTC, there was an increase in the upper layer currents from about 0.25 m s^{-1} to 0.75 m s^{-1} . This change in momentum, combined with the integrated value of the surface momentum flux over the 3 h period ($\sim 2.5 \times 10^4 \text{ Nt-s m}^{-2}$), implies that the momentum supplied by the wind was distributed over an effective depth of 50 m. This value matches the observed mixed layer depth based on density. The upper ocean currents observed at KEO slowed to about 0.55 m s^{-1} by about 1200 UTC on 20 September. Presumably, the primary cause of this decrease was the transfer of energy to the thermocline [Price, 1983]. The mixed layer currents remained of near constant amplitude until late on 25 September and then decreased to $\sim 0.35 \text{ m s}^{-1}$ over the course of about 12 h. In summary, the strong northwesterly winds that occurred immediately after the passage of the center of Choi-Wan represented a source of impulsive forcing of mixed layer currents. The strength of these northwesterlies, relative to the preceding east-northeasterlies, can be attributed to the asymmetry of the cyclone as it passed

KEO. An important result from this case is that wind forcing by a passing tropical cyclone can generate energetic inertial oscillations even on the left side of the storm center's path.

4. Comparison With Other Studies

[18] A set of parameters characterizing Choi-Wan is presented in Table 1. Relative to the events studied by Price *et al.* [1994], Dickey *et al.* [1998] and Shay *et al.* [1998], Choi-Wan was a faster-moving storm and larger, as gauged by the radius of maximum winds R_{MAX} , as it passed KEO. It had comparable values for the maximum wind stress curl (τ_{MAX}) and nondimensional storm speed (S), and for the amplitudes of the maximum ML currents ($\sim 0.8 \text{ m s}^{-1}$) and isopycnal displacements. The latter's value of 12–15 m is consistent with the vertical velocity in the wake of the storm in the formalism of Greatbatch [1984], but is about triple the value suggested by the scaling of Price *et al.* [1994]. The vertical displacements of the isotherms at depth immediately after the storm are consistent with the vertical structure in association with inertial pumping accompanying large, fast moving storms [Greatbatch, 1984]. The mixed layer currents had a maximum amplitude of $\sim 0.8 \text{ m s}^{-1}$. This amplitude is about 80% of the value of U_{ML} indicated from the scaling of Price *et al.* [1994]. This discrepancy is presumably due to the lack of resonance between the rotations of the winds and currents in the present case.

[19] Previous studies of the effect of tropical cyclones on CO_2 gas exchanged have noted a decrease in surface water $p\text{CO}_2$ after the storm [Bates *et al.*, 1998a, 1998b; Nemoto *et al.*, 2009]. In the case of the Bates *et al.* studies, they were not able to sample the area until 6 days after the passage of Hurricane Felix. They noted lower $p\text{CO}_2$ values in the cold wake of the storm, which they attribute to a thermodynamic response to the cooling. On the basis of our observations of the high CO_2 signal, they could have easily missed a mixing signal directly associated with the storm. In fact, a PMEL MAP CO_2 system mounted on the BTM recorded a similar sharp increase followed by a sudden decrease in surface water $p\text{CO}_2$ as a category 2 hurricane, Felix, passed over the BTM in September 2006 (not shown).

[20] Nemoto *et al.* [2009] did have high frequency moored CO_2 observations as the typhoons passed, but saw a decrease in CO_2 values with two of the typhoons and only a modest increase in CO_2 with one typhoon (T9719, which passed well to the right of the measurement location). They did see an increase in temperature normalized $p\text{CO}_2$, however, suggesting that there was entrainment of some high CO_2 water into the mixed layer, but the thermodynamic

Table 1. Scale Parameters for Choi-Wan in the Vicinity of Kuroshio Extension Observatory

Parameter	Value
U_H	11 m s^{-1}
R_{MAX}	90 km
τ_{MAX}	3.3 Nt m^{-2}
$\Delta p\text{CO}_{2\text{MAX}}$	$55 \text{ } \mu\text{atm}$
f	$7.8 \times 10^{-5} \text{ s}^{-1}$
Inertial period	$8.1 \times 10^4 \text{ s}$
$S = \pi U/4fR_{\text{MAX}}$	1.2
$\text{MLD}_{\text{initial}}$	50 m

cooling effect overpowered the signal to give a net decrease in $p\text{CO}_2$.

5. Conclusions

[21] Typhoons cross 30°N between Japan and 155°W an average of once every two weeks during the months of September and October [Bond *et al.*, 2010]. Because they are relatively frequent and cause substantial responses along broad swaths (Figure 1), they represent an important feature of the regional oceanography and potentially the larger climate system. The KEO buoy suffered some damage from the passage of Typhoon Choi-Wan on 19 September 2009, but all variables continued to be measured over the course of the event and its aftermath, and returned a very interesting set of measurements in real time.

[22] The observations of mixed layer (ML) temperature indicate the most rapid cooling after the period of greatest positive wind stress curl/Ekman pumping. Instead, this cooling was associated with combination of upwelling, as revealed by doming of the isotherms and isohalines, and enhanced entrainment, as indicated by the rapid increase in $p\text{CO}_2$ in surface waters. The salinity in the ML increased during the passage of the storm and its aftermath; the fluctuations in the salinity after storm passage appear to be related because of near-inertial currents acting on horizontal gradients in salinity. The near-inertial waves had currents as large as $\sim 0.8\text{ m s}^{-1}$ in the ML and pycnocline displacements of 12–15 m in the seasonal thermocline. These values are comparable to those observed in previous typhoons even though the present case involved cyclonic turning of the winds, and hence a lack of any resonance with the ML near-inertial currents, which rotate anticyclonically. Instead, this was a case of impulsive forcing, due in part to the axial asymmetry in Choi-Wan while in the vicinity of KEO. The STMW below the seasonal thermocline underwent a noticeable, and rather sudden, increase in thermal stratification with the passage of the typhoon. Prominent vertical displacements in the isotherms were observed as deep as 400 m immediately after the storm, and continued over the next 6–7 days.

[23] The full data set from KEO is not yet available. In particular, the ADCP-based currents, and 10 min thermodynamic data that will be forthcoming should allow better characterization of the flow during and in the immediate aftermath of the storm. All of the measurements for this case will be made available to the oceanographic community. While we do not expect these additional measurements to change our findings, they would be helpful in the evaluation of heat, salinity, and momentum budgets and for other kinds of analyses. Our analysis focuses on the data from the KEO mooring. There are other observable assets for the region, namely satellites and floats. These data, however, generally do not have sufficient temporal resolution to capture the evolution of the ocean response to the passage of the typhoons. The generation [Zhai *et al.*, 2007] and propagation [Lee and Niiler, 1998] of near-inertial waves are sensitive to the mesoscale structure of the background fields. The effects of the mesoscale variability are perhaps best diagnosed through high-resolution numerical ocean model experiments. In general, this case represents one of the best data sets in existence for validating numerical ocean model

simulations of the high-frequency aspects of the ocean's response to a strong forcing event.

Appendix A: The Kuroshio Extension Observatory (KEO) Mooring

[24] The Kuroshio Extension Observatory (KEO) mooring deployed in 2009 had several important differences from the KEO mooring described by Cronin *et al.* [2008]. In 2007 the mooring was updated to make it more robust to the harsh conditions of the Kuroshio Extension. In particular, the filled toroid buoy hull was replaced with a 2.5 m discus buoy hull to provide increased buoyancy and improved hydrodynamics to reduce drag. The mooring system was also enhanced with a secondary (duplicate) meteorological sensor suite with a separate data logger (referred to as FLEX). All surface meteorological data are now hourly averaged with a trapezoidal filter centered at the top of the hour and telemetered to shore via Iridium. Likewise, this new data logger telemeters subsurface hourly data to shore via Iridium. In addition, beginning in 2008, the KEO mooring was enhanced with a Druck barometer and a new Vaisala WXT-520 weather module. During typhoon Choi-Wan, the primary meteorological system failed and shortly thereafter, the secondary Gill sonic anemometer failed, leaving the Vaisala WXT-520 as the sole functioning wind sensor. The data used in this study thus relies upon merged data from the primary and secondary systems with corrections as described below.

[25] Intercomparisons between the sensors from the different systems during common functioning periods indicated close agreement for most parameters, with the exception of wind and rain. Both the secondary Gill sonic anemometer and the Vaisala WXT-520 were at lower heights than the primary Gill sonic anemometer and thus were subject to shielding. Consequently, their measured wind speeds were systematically low and required a 10% correction. For rainfall, the primary and secondary R.M. Young gauges agreed remarkably well with one another. Low catchment because of wind is a known problem [Koschmieder, 1934] with rain gauges of the R.M. Young type, hence these data have been corrected using the polynomial provided by Serra *et al.* [2001]. The rain rates measured by the Vaisala WXT-520, however, were about 30–50% higher than these corrected values prior to the typhoon and nearly six times larger during the typhoon, with a peak hourly rate of $\sim 100\text{ mm h}^{-1}$. The Vaisala rain rates are likely too high [Lanza *et al.*, 2010]; we speculate that this may be due to artificially high velocities and hence impacts of raindrops in strong winds. Thus for this study, we use the corrected R. M. Young rain gauge data (Figure 3).

[26] In summary, several changes were made to the KEO mooring system in 2007 that proved to be critical for obtaining observations of Typhoon Choi-Wan. These changes include use of a more stable hull, redundant meteorological sensors, and telemetry of the hourly surface and subsurface data.

[27] **Acknowledgments.** This publication is funded by the NOAA Climate Programs Office and by the Joint Institute for the Study of the Atmosphere and Ocean (JISAO) under NOAA Cooperative Agreement NA17RJ1232, Contribution 1811. The authors wish to thank the captains and crews of the research vessels *Kaiyo*, *Mirai*, and *Kaiyo Maru 5* for their

assistance deploying, repairing, and recovering this mooring. We also thank the engineering and science support staff at PMEL for their continued work developing and operating the KEO buoy and two anonymous reviewers for their constructive comments. This is Pacific Marine Environmental Laboratory Contribution 3529.

References

- Bates, N. R., A. H. Knap, and A. F. Michaels (1998a), Contribution of hurricanes to local and global estimates of air-sea exchange of CO₂, *Nature*, **395**, 58–61, doi:10.1038/25703.
- Bates, N. R., T. Takahashi, D. W. Chipman, and A. H. Knap (1998b), Variability of pCO₂ on diel to seasonal timescales in the Sargasso Sea near Bermuda, *J. Geophys. Res.*, **103**, 15,567–15,585, doi:10.1029/98JC00247.
- Bender, M. A., I. Y. Ginis, and Y. Kurihara (1993), Numerical simulations of tropical cyclone-ocean interaction with a high-resolution coupled model, *J. Geophys. Res.*, **98**, 23,245–23,263, doi:10.1029/93JD02370.
- Bond, N. A., M. F. Cronin, and M. Garvert (2010), Atmospheric sensitivity to SST near the Kuroshio Extension during the extratropical transition of Typhoon Tokage, *Mon. Weather Rev.*, **138**(7), 2644–2663, doi:10.1175/2010MWR3198.1.
- Cronin, M. F., C. Meinig, C. L. Sabine, H. Ichikawa, and H. Tomita (2008), Surface mooring network in the Kuroshio Extension, *IEEE Syst. J.*, **2**(3), 424–430.
- D'Asaro, E. A., T. B. Sanford, P. P. Niiler, and E. J. Terrill (2007), Cold wake of Hurricane Frances, *Geophys. Res. Lett.*, **34**, L15609, doi:10.1029/2007GL030160.
- Dickey, T., D. Frye, J. McNeil, D. Manov, N. Nelson, D. Sigurdson, H. Jannasch, D. Siegel, T. Michaels, and R. Johnson (1998), Upper-ocean temperature response to Hurricane Felix as measured by the Bermuda Testbed Mooring, *Mon. Weather Rev.*, **126**, 1195–1201, doi:10.1175/1520-0493(1998)126<1195:UOTRTH>2.0.CO;2.
- Emanuel, K. (2001), Contribution of tropical cyclones to meridional heat transports by oceans, *J. Geophys. Res.*, **106**, 14,771–14,781, doi:10.1029/2000JD900641.
- Fairall, C. W., E. F. Bradley, J. E. Hare, A. A. Grachev, and J. B. Edson (2003), Bulk parameterization of air-sea fluxes: Updates and verification for the COARE algorithm, *J. Clim.*, **16**, 571–591, doi:10.1175/1520-0442(2003)016<0571:BPOASF>2.0.CO;2.
- Gill, A. E. (1984), On the behavior of internal waves in the wakes of storms, *J. Phys. Oceanogr.*, **14**, 1129–1151, doi:10.1175/1520-0485(1984)014<1129:OTBOIW>2.0.CO;2.
- Greatbatch, R. J. (1984), On the response of the ocean to a moving storm: Parameters and scales, *J. Phys. Oceanogr.*, **14**, 59–78, doi:10.1175/1520-0485(1984)014<0059:OTROTO>2.0.CO;2.
- Hanawa, K., and T. Suga (1995), A review on the subtropical mode water of the North Pacific (NPSTMW), in *Biogeochemical Processes and Ocean Flux in the North Pacific*, edited by H. Sakai, Y. Nozaki, pp. 613–627, Terra Sci., Tokyo.
- Jacob, S. D., L. K. Shay, and A. J. Mariano (2000), The 3D oceanic mixed layer response to Hurricane Gilbert, *J. Phys. Oceanogr.*, **30**, 1407–1429, doi:10.1175/1520-0485(2000)030<1407:TOMLRT>2.0.CO;2.
- Kako, S., and M. Kubota (2007), Variability of mixed layer depth in Kuroshio/Oyashio Extension region: 2005–2006, *Geophys. Res. Lett.*, **34**, L11612, doi:10.1029/2007GL030362.
- Koschmieder, H. (1934), Methods and results of definite rain measurements, *Mon. Weather Rev.*, **62**, 5–7, doi:10.1175/1520-0493(1934)62<5:MARODR>2.0.CO;2.
- Kubota, M., N. Iwabe, M. F. Cronin, and H. Tomita (2008), Surface heat fluxes from the NCEP/NCAR and NCEP/DOE reanalyses at the KEO buoy site, *J. Geophys. Res.*, **113**, C02009, doi:10.1029/2007JC004338.
- Lanza, L. G., E. Vuerich, and I. Gnecco (2010), Analysis of highly accurate rain intensity measurements from a field test site, *Adv. Geosci.*, **25**, 37–44, doi:10.5194/adgeo-25-37-2010.
- Lee, D., and P. Niiler (1998), The inertial chimney: The near-inertial energy drainage from the ocean surface to the deep layer, *J. Geophys. Res.*, **103**, 7579–7591, doi:10.1029/97JC03200.
- Maeda, A., K. Uejima, T. Yamashiro, M. Sakurai, H. Ichikawa, M. Chaen, K. Taira, and S. Mizuno (1996), Near inertial motion excited by wind change in a margin of the Typhoon 9019, *J. Oceanogr.*, **52**, 375–388, doi:10.1007/BF02235931.
- Marks, F. D., D. Atlas, and P. T. Willis (1993), Probability-matched reflectivity-rainfall relations for a hurricane from aircraft observations, *J. Appl. Meteorol.*, **32**, 1134–1141, doi:10.1175/1520-0450(1993)032<1134:PMRRRF>2.0.CO;2.
- McPhaden, M. J., G. R. Foltz, T. Lee, V. S. N. Murty, M. Ravichandran, G. A. Vecchi, J. Vialard, J. D. Wiggert, and L. Yu (2009), Ocean-atmosphere interactions during Cyclone Nargis, *Eos Trans. AGU*, **90**(7), doi:10.1029/2009EO070001.
- Nemoto, K., T. Midorikawa, A. Wada, K. Ogawa, S. Takatani, H. Kimoto, M. Ishii, and H. Y. Inoue (2009), Continuous observations of atmospheric and oceanic CO₂ using a moored buoy in the East China Sea: Variations during the passage of typhoons, *Deep Sea Res., Part II*, **56**(8–10), 542–553, doi:10.1016/j.dsr2.2008.12.015.
- Price, J. F. (1983), Internal wave wake of a moving storm. Part I: Scales, energy budget and observations, *J. Phys. Oceanogr.*, **13**, 949–965, doi:10.1175/1520-0485(1983)013<0949:IWVOAM>2.0.CO;2.
- Price, J. F., T. B. Sanford, and G. Z. Forristall (1994), Forced stage response to a moving hurricane, *J. Phys. Oceanogr.*, **24**, 233–260, doi:10.1175/1520-0485(1994)024<0233:FSRTAM>2.0.CO;2.
- Qiu, B., and S. Chen (2006), Decadal variability in the formation of the North Pacific subtropical mode water: Oceanic versus atmospheric control, *J. Phys. Oceanogr.*, **36**, 1365–1380, doi:10.1175/JPO2918.1.
- Sanford, T. B., P. G. Black, J. Haustein, J. W. Fenney, G. Z. Forristall, and J. F. Price (1987), Ocean response to hurricanes, Part I: Observations, *J. Phys. Oceanogr.*, **17**, 2065–2083.
- Serra, Y. L., P. A'Hearn, H. P. Freitag, and M. J. McPhaden (2001), ATLAS self-siphoning rain gauge error estimates, *J. Atmos. Oceanic Technol.*, **18**, 1989–2002, doi:10.1175/1520-0426(2001)018<1989:ASSRGE>2.0.CO;2.
- Shay, L. K., A. J. Mariano, S. D. Jacob, and E. H. Ryan (1998), Mean and near-inertial ocean current response to Hurricane Gilbert, *J. Phys. Oceanogr.*, **28**, 858–889, doi:10.1175/1520-0485(1998)028<0858:MANIOC>2.0.CO;2.
- Shellito, S., J. Irish, D. Vandemark, S. Maenner, N. Lawrence-Slavas, and C. Sabine (2008), Time-series measurements of atmospheric and ocean CO₂ and O₂ in the western Gulf of Maine, paper presented at Oceans 2008 Conference, Quebec City, Quebec, Canada, 15–18 September 2008.
- Sriver, R. L., and M. Huber (2010), Modeled sensitivity of upper thermocline properties to tropical cyclone winds and possible feedbacks on the Hadley circulation, *Geophys. Res. Lett.*, **37**, L08704, doi:10.1029/2010GL042836.
- Takahashi, T., J. Olafsson, J. G. Goddard, D. W. Chipman, and S. C. Sutherland (1993), Seasonal variation of CO₂ and nutrients in the high-latitude surface oceans: A comparative study, *Global Biogeochem. Cycles*, **7**, 843–878, doi:10.1029/93GB02263.
- Zhai, X., R. J. Greatbatch, and C. Eden (2007), Spreading of near-inertial energy in a 1/12° model of the North Atlantic Ocean, *Geophys. Res. Lett.*, **34**, L10609, doi:10.1029/2007GL029895.

N. A. Bond and K. Ronnholm, Joint Institute for the Study of the Atmosphere and Ocean, Box 354925, University of Washington, Seattle, WA 98195-4925, USA. (nab3met@u.washington.edu)

M. F. Cronin, P. Freitag, and C. Sabine, Pacific Marine Environmental Laboratory, NOAA, 7600 Sand Point Way NE, Seattle, WA 98115, USA.
H. Ichikawa and Y. Kawai, Japan Agency for Marine-Earth Science and Technology, Yokosuka, Japan.